



THE UNIVERSITY *of* EDINBURGH
Edinburgh Medical School

Biomedical Sciences

Title of Assessment:
NEBM11002 – Masters Dissertation

Examination Number:

B243063

Please use this number as your “Submission Title” in Learn when you submit your essay online.

Course Name:
MScR Integrative Neuroscience

Word count:
Abstract – 242 words
Main Text – 6,335 words

MScR Integrative Neuroscience

Master's Dissertation

Internal representations of space in the
visual cortex during a goal-directed task
in the dark

Examination Number:

B243063

August 2024

Acknowledgement

I would like to express my gratitude towards Professor Nathalie Rochefort for her guidance, advice, encouragement, and for being a good leadership role model.

I would also like to thank Dr. Nina Kudryashova and Dr. Alfredo Llorca Molina for their continuous support in helping me develop a deeper insight about the project and relevant research skills.

The past few months have shown me a glimpse of what a career in research is like and it has been my pleasure to have the opportunity to work alongside the members of the Lab.

Contents

Acknowledgement

Contents

Abstract

1. Introduction

1.1. Internal representations and predictive decoding	1
1.2. Integrating spatial representations in the absence of visual inputs	2
1.3. Calcium imaging data of V1 neural activity during navigation in virtual reality	3
1.4. Challenges in decoding spatial representation from V1 neural activity	4
1.5. Decoding with Bayesian Inference	6
1.6. Project Aim and Objectives	7

2. Methods

2.1. Overview of data structure and pre-processing	8
2.1.1. Behavioural task details	8
2.1.2. Calcium imaging and data extraction	8
2.1.3. Data pre-processing	9
2.2. Deriving spatial tuning curves	10
2.3. Developing Bayesian Decoder	11
2.3.1. Bayes' Theorem	11
2.3.2. Decoder function	11
2.3.3. Training and Testing Paradigms	12
2.4. Evaluation of the Bayesian Decoder performance	13
2.4.1. Confusion matrix	13
2.4.2. Accuracy and errors	13
2.4.3. Benchmarking against maximum likelihood decoder	14

3. Results

3.1. Spatial Tuning Curves	15
3.2. Bayesian Decoder Performance	18
3.2.1. Assessing the presence of spatial representation in V1	18
3.2.2. Assessing similarity and differences between the spatial neural code in light and dark	20
3.2.3. Evaluating certainty of the decoder	22
3.3. Results Conclusion	23

4. Discussion

4.1. Advantages and limitations of Bayesian Decoder	24
4.1.1. Advantages of adopting Bayesian inference	24
4.1.2. Limitations and optimisation for decoder	24
4.2. Decoder performance and spatial neural code	25
4.2.1. Spatial representation in mouse V1 in light and dark	25
4.2.2. Sharing of spatial neural code between light and dark	26
4.3. Future direction: application to large-scale electrophysiological recordings	27

References

Abstract

Reliable spatial representations generated from the hippocampus are important for successful navigation and survival. Previous studies have shown that these top-down spatial representations are encoded in the primary visual cortex (V1) and integrated with bottom-up sensory inputs. However, whether and how V1 maintains these spatial representations in the absence of visual cues remains unknown.

In addressing this research gap, members of the Rochefort Lab utilised a virtual reality navigation task with two-photon calcium imaging to investigate the spatial neural code of mouse V1 in light and dark. It is hypothesised that V1 encodes spatial representations in both light and dark conditions when visual cues are absent.

To test the hypothesis, this thesis developed a decoder based on Bayesian inference to predict the spatial location of the mouse from its V1 neural response. The probabilistic framework of the Bayesian decoder is known to be advantageous in handling noise and uncertainty in the data, thus making it a suitable choice as a decoding methodology. Decoding results showed that the decoder's prediction outperformed chance level estimates in light, and to a smaller degree, in the dark.

The current results offered preliminary support to the hypothesis that spatial representations are encoded in V1 both when the sensory inputs are present, and when they are absent. While it requires further optimisation, the Bayesian decoder is a promising tool that can be applied to datasets from electrophysiological recordings, which would allow more robust testing of the hypothesis.

1. Introduction

Accurate and reliable sensory perceptions are essential for survival. It has previously been shown that sensory cortices use top-down internal information from higher cortical areas to predict sensory input and integrate this information with sensory cues (Barrett and Simmons, 2015; Clark, 2013; Friston, 2005; Keller and Mrsic-Flogel, 2018; Rao and Ballard, 1999). In the primary visual cortex (V1), this integration occurs not only for basic features of visual stimuli, such as orientation, depth, and colour, but also for complex stimuli, like the unique combination of visual features that reflects the spatial location of the animal in the environment (Fiser et al., 2016; Pakan et al., 2018; Saleem et al., 2018).

Reliable spatial representations are critical as they help the animal locate resources and avoid dangers while navigating in familiar territory. When visual cues are lacking in the dark, internal representations of the familiar environment become especially important. However, how these internal representations of the environment are recruited in the absence of visual cues and whether this spatial information propagates down to the primary visual cortex remains unclear.

This thesis is part of a project that aims to determine the cortical circuits encoding spatial representations of a familiar environment when animals navigate in the absence of visual cues. A key point of this project is to assess whether V1 neural network responses encode information about this familiar environment when visual cues are not visible. This thesis aims to develop a Bayesian decoding methodology that would reveal and characterise the encoding of spatial information in mouse V1 activity. This decoding approach was applied to V1 neuronal responses of mice performing a virtual reality (VR) navigation task. V1 neuronal responses were recorded using two-photon calcium imaging. The results of my analysis establish the role of V1 in encoding internally generated representations when sensory information is unavailable.

1.1. Internal representations and predictive decoding

An internal model is what the brain uses when it tries to make sense of the external reality we live in. Sometimes, these models are used to construct internal representations, which can take the form of a happy memory, an imagined future scenario, or

the cognitive map of a familiar environment. They help us learn from our past and plan better actions optimising for future rewards. In other cases, however, internal models also reflect more subtle models of the statistical regularities in the sensory world. Some good examples include the likelihood of having a shadow beneath an object instead of above, or that moving objects on a highway are more likely to be cars than boats. While we often take these internal models of the world for granted, they are the cornerstone of the predictive coding framework of perception.

In the last two decades, predictive coding has gained much traction as a widely adopted theoretical framework for perception (Barrett and Simmons, 2015; Clark, 2013; Friston, 2005; Keller and Mrsic-Flogel, 2018; Rao and Ballard, 1999). Within this framework, the brain is constantly using its internal models of the world to make predictions about what is most likely to happen next in the external reality. The brain then compares these top-down predictions with the actual sensory inputs it receives. In cases where the top-down predictions contradict the sensory inputs, *i.e.* a prediction error occurs, the brain would then refine the internal models to minimise the prediction error.

When sensory inputs are reliable, expectations can improve the efficiency, sensitivity, and accuracy of perceptions (de Lange et al., 2018). On the other hand, if sensory inputs are noisy and ambiguous, for example when an image is partially occluded, top-down spatial expectations become more prominent and will bias visual perceptions more strongly (de Lange et al., 2018).

1.2. Integrating spatial representations in the absence of visual inputs

Sensory cortices can be active even if there are no sensory inputs as they can still receive and integrate representations from higher cortical areas. In humans, for example, primary sensory areas are activated in mental navigation and mental imagery when sensory inputs are absent (Gramann et al., 2010; Huang and Sereno, 2013; Kober et al., 2014).

To understand how the mechanisms work at the circuitry and cellular level, rodent models are very useful given the availability of recording methods and genetic tools. Recent findings (see review, Flossmann and Rochefort, 2021) have shown that the mouse primary visual cortex (V1) also integrates top-down expectations from higher

cortices. This includes navigation-related signals such as locomotion (*i.e.* speed), distance travelled, head orientation, as well as spatial representations of the animals' location (Fiser et al., 2016; Pakan et al., 2018; Saleem et al., 2018).

These spatial representations are known to be encoded by hippocampal place cells (Flossmann and Rochefort, 2021; O'Keefe and Conway, 1978) and are pre-played when planning for future journeys from a starting location to a destination (Pfeiffer and Foster, 2013). The spatial representations may then propagate to sensory cortical areas including V1, likely through the medial entorhinal cortex (MEC) and retrosplenial cortex (RSC). The MEC is considered a candidate area for conveying spatial representations to V1 as previous evidence has shown that it is critical for predicting future spatial location (Campbell et al., 2021), path integration (McNaughton et al., 2006) and pre-play of place cell activity (O'Neill et al., 2017). Meanwhile, the RSC has been shown to integrate locomotion and visual signals (Fischer et al., 2020; Mao et al., 2020), and to encode spatial location through ramping activity (Tennant et al., 2022). In addition, deep layers of MEC receive input from the hippocampus and RSC, and project outputs to higher cortical areas (Gerlei et al., 2021).

Although there is evidence that MEC and RSC are important for navigation in the absence of sensory information in the dark (Campbell et al., 2021; Elduayen and Save, 2014), their involvement in conveying internal spatial information to V1 in such circumstances remains unclear.

1.3. Calcium imaging data of V1 neural activity during navigation in virtual reality

To study the circuits encoding internal representations of familiar environments in the absence of visual cues, one must begin by assessing whether spatial representations are encoded in V1 in the presence and absence of visual cues ('light' and 'dark' conditions). Llorca et al. from the Rochefort Lab used a virtual reality (VR) experimental paradigm, which allows the experimenter to have full control over the visual stimuli presented to the animals.

Head-fixed mice were placed into a virtual environment, where they were trained to navigate a 500 cm corridor with visual landmarks (Figure 1). The mice could get a reward by licking a spout at a specific location in the corridor as indicated by visual cues. To ensure that the mice rely on landmarks to navigate (allocentric navigation, as

opposed to egocentric navigation), they were trained to start each trial at a random location in the tunnel.

When the mice had learnt the task successfully, 40% of the trials introduced a ‘dark’ condition, where the mice could only see the first 50 cm of the tunnel, and they would have to navigate to the reward zone in the dark with no visual cues or landmarks. Two-photon calcium imaging was used to record the neural activity of the mice V1 layer 2/3 excitatory neurons before, during and after the learning of the task, both in light and dark trials.

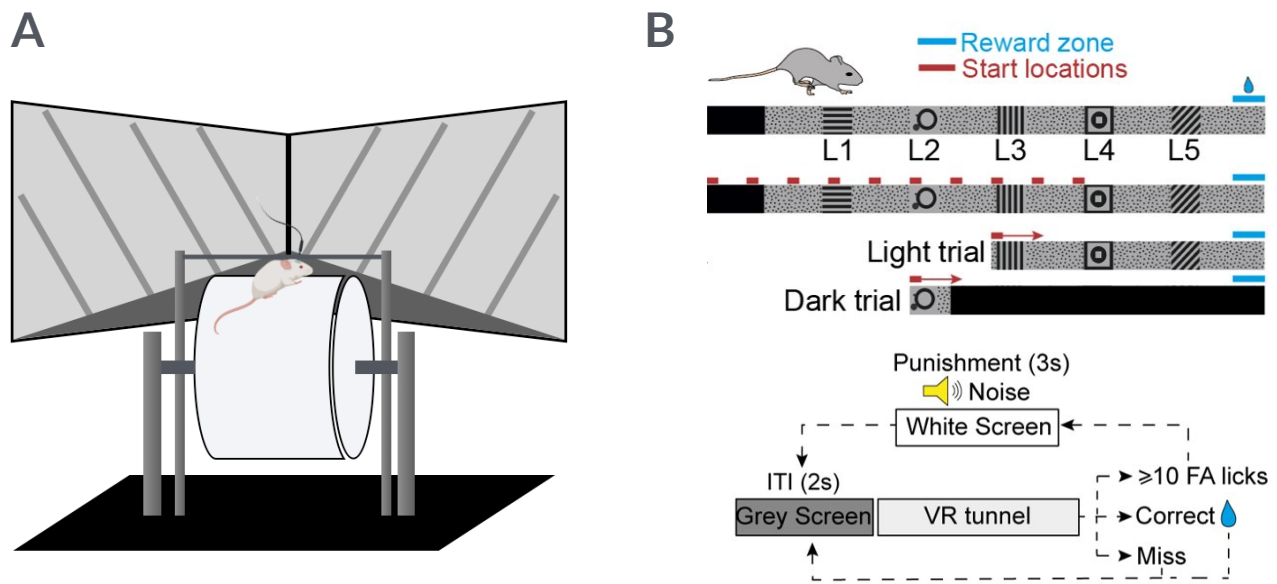


Figure 1: Virtual Reality Navigation Task

(A) Virtual reality set up. **(B)** Task structure. Head-fixed mice navigate a 500cm virtual tunnel. Mice can trigger a water reward by licking in the reward zone (blue). The animal’s starting point in each trial is pseudo-randomized (red). During training and light trials, the whole tunnel is visible. In dark trials, only the first 50cm is visible, after which the virtual tunnel becomes all black. Only licks inside the reward zone trigger a reward, licks within 50cm before the reward zone are considered hit, and licks before that are considered false alarms (FA). A 2s inter-trial-interval (ITI) showing a grey screen precedes each trial. 10 or more FA licks in one trial lead to trial abortion and a 3s time out punishment, paired with a white screen and an aversive noise.

1.4. Challenges in decoding spatial representation from V1 neural activity

Determining spatial representation in V1 neural activity requires methods to retrieve spatial information from neural responses. Decoding methods can be employed to achieve this goal. To “decode” is to find a mapping between neural data and the sensory stimuli presented to the animal (van der Meer et al., 2017) and to reconstruct the

stimuli from the neural data (Zhang et al., 1998). In other words, if there is spatial information in V1 neural activity, a decoder should be able to predict the spatial location of the animal from the neuronal activity.

There are, however, multiple challenges in decoding spatial representation from V1 neural activity. First, it is known that only a small fraction of neurons in mouse V1 are spatially tuned, which makes it difficult for the decoders to reconstruct spatial representations as they typically become less accurate with fewer spatially-selective neurons to decode from. Second, V1 activity tends to be lower in dark than in light, this adds challenges to the decoder separating signal from noise.

There are also obstacles imposed by the recording method. Calcium imaging, like many other recording methods, is not a direct measure of neuronal spikes, but rather an indirect approximation of neural activity. Fluorescent calcium indicators change their fluorescence intensity when they bind to calcium ions. Since neuronal responses are linked to an increase in intracellular calcium levels, calcium imaging exploits these dynamics to capture changes in neural activity and is used as a proxy for action potentials. However, the rising time of these fluorescent indicators (*e.g.* GCamp6s) is in the range of hundreds of milliseconds (Kwan et al., 2010), and their decay time is in the range of seconds, which does not offer a very good temporal resolution for the neural activity that occurs at a millisecond time scale. As such, neuronal spikes cannot be directly measured with calcium imaging. For analysis methods requiring binary signals (spikes), firing rates can be inferred from calcium levels. This spike inference can be done through established analysis pipelines (*e.g.* CASCADE, established by Helmchen lab, Rupprecht et al., 2021). Although these methods have been optimised to best capture neuronal spiking, some information might be lost during the process.

Finally, the experimental design itself also adds complexity to decoding. Given that each trial has a randomised start location in the tunnel, the probability for the mouse to occupy a certain location in the tunnel can be different across trials. Additionally, two different experimental conditions (light and dark trials) further reduce the amount of data available for analysis, especially for dark trials which only account for 40% of total trials.

1.5. Decoding with Bayesian Inference

In addressing the above challenges, this thesis proposed to develop a Bayesian decoder to decode the spatial representations from mouse V1 neural activity.

There have been various approaches trying to tackle the challenges inherent to calcium imaging decoding, such as the use of linear discriminant analysis (Lee et al., 2017), support vector machine (Lee et al., 2019; Lee et al., 2020; Sun et al., 2023), visibility graph (Zhu et al., 2018), multilayer perceptron (Sun et al., 2023), and long short-term memory decoder (Sun et al., 2023). More recently, when testing a strategy to extract features from calcium traces without spike inference (Tu et al., 2020), researchers have also used maximum likelihood estimation (MLE) and optimal linear estimation. While there is no consensus as to which decoder is “best” given the different characteristics of different datasets, Bayesian inference has remained a popular option for calcium image decoding (Etter et al., 2020; Gobbo et al., 2022; Saleem et al., 2018; Sun et al., 2023; Tu et al., 2020).

Bayes’ Theorem:

$$P(x|n) = \frac{P(n|x)P(x)}{P(n)}$$

The proposed Bayesian decoder would use Bayes’ Theorem as a framework behind the computation. To decode spatial representations, it would take in prior information about the neural activity and spatial representations and return a posterior probability estimating the most likely location of the mice that elicited the particular pattern of neural activity.

Bayesian inference is an advantageous decoding method for addressing the aforementioned decoding challenges as its probabilistic framework allows the decoder to handle noise and uncertainty in the data. It also provides a measure of the decoder’s “confidence” in its predictions, which makes it possible for researchers to evaluate the quality of decoder predictions. The prior can also allow the incorporation of various hypotheses into the decoding analysis, and the right prior can improve decoder accuracy. For instance, we can assume that in shorter trials, V1 would not represent any location before the start of the trial, and this information can be incorporated into the model by modifying the prior of the decoder.

The proposed decoder would adopt a Poisson likelihood function for estimating the likelihood of neural activity given spatial location. Poisson likelihood is favoured in this case over other commonly used likelihood functions (*e.g.* Gaussian) because it offers a good fit to spikes data which are discrete by nature. It has been used previously by Grosmark and Buzsaki (2016) in decoding hippocampal dynamics.

Even though the choice of Poisson likelihood means that spike inference has to be done on the calcium imaging data we have currently, it gives the possibility to use this decoder for analysing future experimental data acquired by electrophysiological recordings (*e.g.* from large-scale Neuropixels recordings) with higher (ms) temporal resolution.

1.6. Project Aim and Objectives

Under the overarching goal of investigating the cortical circuits encoding internal representations of a familiar environment in the absence of visual inputs, this thesis project aims to determine whether there are spatial representations encoded in the mouse V1 neural activity in the absence of sensory inputs through the development and implementation of a Bayesian decoder. I will test the hypothesis that V1 neurons encode spatial representations in the dark.

In achieving this aim, the following objectives are being set out:

- I. Derive spatial tuning curves from V1 neural activity.
- II. Develop and optimise a Bayesian decoder to determine if spatial neural code exists in V1 when sensory inputs are absent in the dark.
- III. Determine whether and how the spatial neural code in mouse V1 is shared between light and dark trials.

2. Methods

2.1. Overview of data structure and pre-processing

Alfredo Llorca Molina from the Rochefort Lab completed the behavioural experiments (Figure 1) and obtained the calcium imaging data. The V1 neural activity of five expert mice (3 males, and 2 females) was recorded during the virtual reality task described in Section 1.3. In the scope of this thesis project, only data from a single representative mouse in terms of behavioural performance and number of recorded neurons were used in the development of the decoder.

2.1.1. Behavioural task details

Water-restricted mice were navigating a 500 cm virtual reality tunnel which has 5 landmarks and an unlabelled reward zone at the end of the tunnel (Figure 1 and Table 1). The animal was rewarded with water when licked at the reward zone. The starting location of each trial was randomised to prevent the animals from using egocentric navigation, *i.e.* estimating the distance travelled from the start. To test internally-guided navigation, a dark condition was introduced in 30-40% of the trials. In these trials, mice were allowed to see the tunnel only at the start to estimate their starting location. After walking 50cm, the tunnel was switched to a dark screen. If animals correctly lick inside the reward zone and trigger a reward, the tunnel is shown again for reinforcement. Each trial was preceded by a 2s grey screen and a sound tone to indicate the start of the trial. Excessive licking outside the reward zone was punished with a 3s timeout coupled with bright white screens and an aversive noise.

2.1.2. Calcium imaging and data extraction

In each experimental session, mice perform the navigation task for 45-60 minutes. During this time, the activity of V1 excitatory neurons was recorded using calcium imaging. The number of neurons recorded per animal was variable, varying between 83 and 142. The single mouse data being used for developing the decoder had 125 recorded neurons and 257 trials.

Table 1: Landmark and reward zone locations in the tunnel

Landmark	Location in Tunnel	Visual Cue
Landmark 1	110 cm - 130 cm	Vertical gratings
Landmark 2	190 cm - 210 cm	Circles
Landmark 3	270 cm - 290 cm	Horizontal gratings
Landmark 4	350 cm - 370 cm	Squares and circles
Landmark 5	440 cm - 460 cm	45-degree gratings
Reward Zone	465 cm - 495 cm	/

Since calcium imaging is only a proxy for neural activity, discrete spikes were inferred from the calcium fluorescence using a previously published convoluted neural network called CASCADE (Rupprecht et al., 2021).

Calcium imaging data of the neural activity was then aligned with the spatial data of the virtual reality tunnel. Since we are only interested in recordings during navigation, the following sections of the data were then pruned: grey screens at the beginning of the trial, punishments, and trial-to-trial transition time. Next, the inferred spikes data was binned in 100 ms time bins, forming a three-dimensional tensor (Neurons x Trials x Time Bins). Mice spatial occupancy was also binned in 100ms time bins. Positions occupied were binned in 10cm bins. Thus, a two-dimensional position matrix was computed (Trials x Time bins) reflecting which 10cm position bin was occupied by the animal during each 100ms temporal bin.

2.1.3. Data pre-processing

To motivate navigation and avoid disengagement from the behavioural task, an automatic reward irrespective of mouse licking was provided in a few trials. Data from such trials was removed from the dataset. To avoid including data from animals that had disengaged from the task or were temporarily distracted, trials in which the animal did not lick at all were also excluded. In the case of the single mouse used for developing the decoder, 13 trials were excluded, yielding 244 trials for further analysis.

To evaluate spatial information encoded in V1 in darkness, we will need to exclude all times when the tunnel is visible from our dark trials, before decoding positional information. Hence, neural activity corresponding to the first 50cm and inside the reward zone (the two times animals can see the tunnel during dark trials) was cropped

out by replacing the numerical values with not-a-number (NaN) values (Figure 2). For consistency, the same procedures were applied in light trials.

A Gaussian smooth was then performed on the inferred spikes matrix with a sigma of two time bins (*i.e.* 200 ms, Figure 2). The smoothed spikes were then split into light and dark trials to be used independently in the decoder.

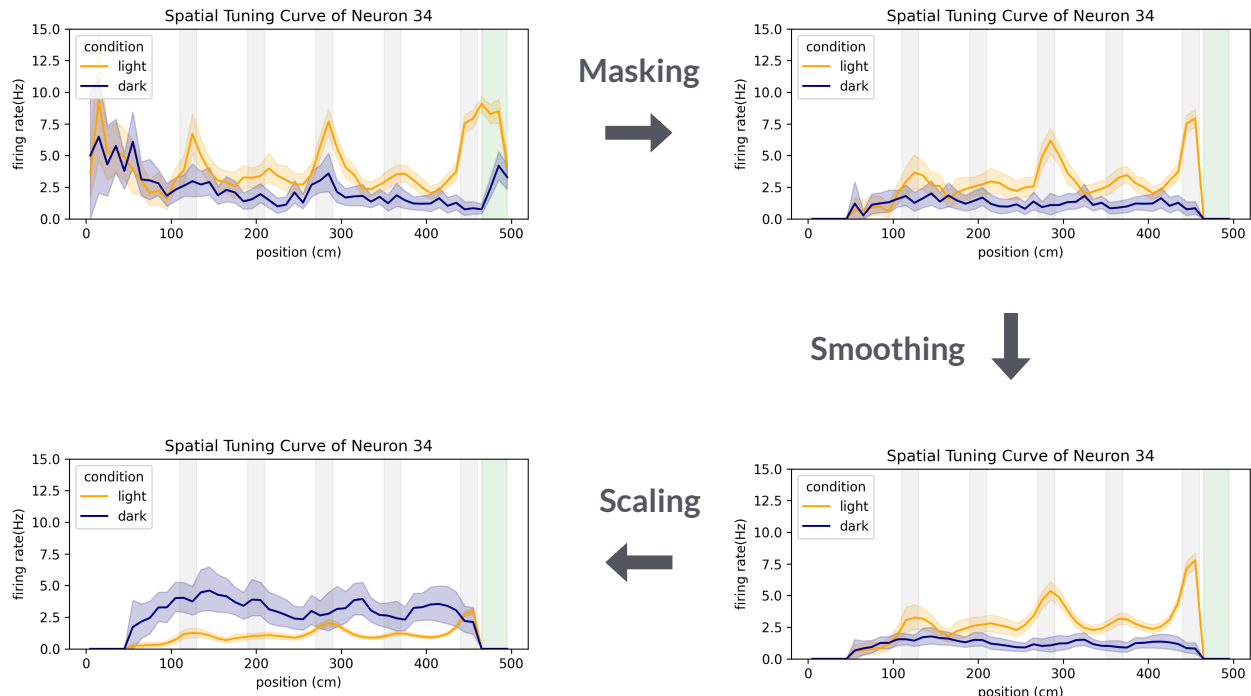


Figure 2: Schematic of the data pre-processing steps

To exclude all times when tunnel is visible to the animal, data corresponding to the first 50 cm of the tunnel and the reward zone were masked with not-a-number (NaN) values. A Gaussian smooth was then applied to the spikes data, with sigma = 200ms. Lastly, the light trial data was scaled with a coefficient calculated by the mean firing rates of light trials divided by the mean firing rates of dark trials, vice versa for dark trials.

2.2. Deriving spatial tuning curves

To derive tuning curves, the animal's occupancy was first computed, *i.e.* for each position bin of the tunnel, the number of time bins the mouse was in that position bin. Then, the smoothed spikes data corresponding to each position bin were summed and divided over occupancy to generate a firing rates matrix (Neurons x Trials x Position Bins). The number of spikes divided by the time spent in a position bin yields a firing rate, which is then plotted to obtain spatial tuning curves.

2.3. Developing Bayesian Decoder

2.3.1. Bayes' Theorem

Bayesian inference is a probabilistic decoding framework. The Bayes Theorem is given:

$$P(x | n) = \frac{P(n | x) P(x)}{P(n)} \quad (1)$$

It asks, “What is the probability of x given the observation n ?“

In this case, posterior $P(x | n)$ is the probability for the mouse to be at position x given the neuron's activity n . $P(x)$ is the spatial prior, $P(n)$ is the probability for spike activity n to occur, and $P(n | x)$ is the likelihood of having neuron's activity n given the mouse is at spatial location x .

For easier computation, we take the log of Bayes' Theorem:

$$\log P(x | n) = \log P(n | x) + \log P(x) - \log P(n) \quad (2)$$

2.3.2. Decoder function

The standard approach (Zhang et al., 1998) was used to decode the spatial location of the mouse, assuming Poisson-distributed spikes around the mean firing rate and independence between neurons. Equation (2) thus can be expanded as follows.

The spatial prior is:

$$P(x) = \frac{1}{\text{number of position bins}} \quad (3)$$

The Poisson likelihood is given:

$$P(n | x) = \prod_{i=1}^N \frac{\lambda_i^{n_i} e^{-\lambda_i}}{n_i!} \quad (4)$$

Where $\lambda = \tau f_i(x)$.

$f_i(x)$ is the average firing rate of neuron i at position x , and τ is the size of the time bin. Taken together:

$$P(n|x) = \prod_{i=1}^N \frac{(\tau f_i(x))^{n_i}}{n_i!} \exp(-\tau f_i(x)) \quad (5)$$

Taking log of $P(n|x)$, we have:

$$\log P(n|x) = \sum_{i=1}^N n_i \log \lambda_i - \lambda_i - \log(n_i!) \quad (6)$$

Finally, the log of the marginal probability is:

$$\log P(n) = \log \sum_{x=1}^X P(n|x)P(x) \quad (7)$$

Essentially, what the decoder does is use the position-binned firing rates matrix $f_i(x)$ as training data (excluding the trial that is being decoded), then, based on the inferred spikes n of each time bin, return a posterior probability distribution $P(x|n)$ for each position bin x . The peak of the probability distribution will be the decoded position for that time bin.

2.3.3. Training and Testing Paradigms

Different training and testing paradigms were used to investigate if the spatial neural code between light trials and dark trials was shared (Table 2). Such can be achieved by training the decoder with light data and decoding dark responses and vice-versa (cross-training).

The average firing rate for light and dark trials could be vastly different for spatially tuned neurons. When the decoder adopted a cross-train paradigm, firing rates were scaled by the mean activity of the trials from the opposite condition.

$$\text{scaled firing rates}_{light} = \text{firing rates}_{light} \times \frac{\text{mean firing rates}_{dark}}{\text{mean firing rates}_{light}} \quad (8)$$

$$\text{scaled firing rates}_{dark} = \text{firing rates}_{dark} \times \frac{\text{mean firing rates}_{light}}{\text{mean firing rates}_{dark}} \quad (9)$$

Table 2: Decoder Training and Testing Paradigms

Train in Light, Test in Light	Feeding position-binned firing rates of light trials to the decoder as training data and decoding the spatial location of mice from spikes data of light trials
Train in Light, Test in Dark	Feeding position-binned firing rates of dark trials to the decoder as training data and decoding the spatial location of mice from spikes data of dark trials
Train in Dark, Test in Dark	Feeding position-binned and scaled firing rates of light trials to the decoder as training data, and decoding the spatial location of mice from spikes data of dark trials
Train in Dark, Test in Light	Feeding position-binned and scaled firing rates of dark trials to the decoder as training data, and decoding the spatial location of mice from spikes data of light trials

2.4. Evaluation of the Bayesian Decoder performance

2.4.1. Confusion matrix

The performance of the decoder would first be evaluated with a confusion matrix. The rows represent the true position of the animal and the columns represent the decoders' predicted positions. The confusion matrix plots for each true position y , the percentage of the decoder's prediction for the position bin x . If the decoded position is accurate, the confusion matrix should show a clear diagonal line.

$$\% = \frac{\text{number of predicted position } x}{\text{total number of predictions for } y} \quad (10)$$

2.4.2. Accuracy and errors

Next, the decoder would be evaluated by accuracy and error measures. Accuracy is measured by the percentage of correct predictions. Error reflects the distance between the decoded position and the occupied position.

$$\text{Accuracy} = \frac{\text{number of correct predictions}}{\text{total number of predictions}} \quad (11)$$

$$\text{Mean Error} = \frac{\sum |\text{decoded position} - \text{actual position}|}{\text{total number of predictions}} \quad (12)$$

2.4.3. Benchmarking against maximum likelihood decoder

Finally, the decoder performance was benchmarked against the performance of a maximum likelihood decoder developed by Llorca from the Rochefort Lab. This comparison aims to reveal if the Bayesian framework is a more suitable option for this dataset.

3. Results

3.1. Spatial Tuning Curves

To evaluate spatial encoding in V1 during navigation in light and dark conditions, we first calculated spatial tuning curves for the recorded V1 neurons. Firing rate tuning curves were calculated from inferred spikes and smoothed using a Gaussian filter. This allows us to examine the spatial tuning profiles of the recorded neurons in mouse V1. Figure 3 shows spatial tuning curves of all neurons in a single mouse ($n = 125$) for light and dark trials respectively. Each line represents a single neuron's average firing rate across trials.

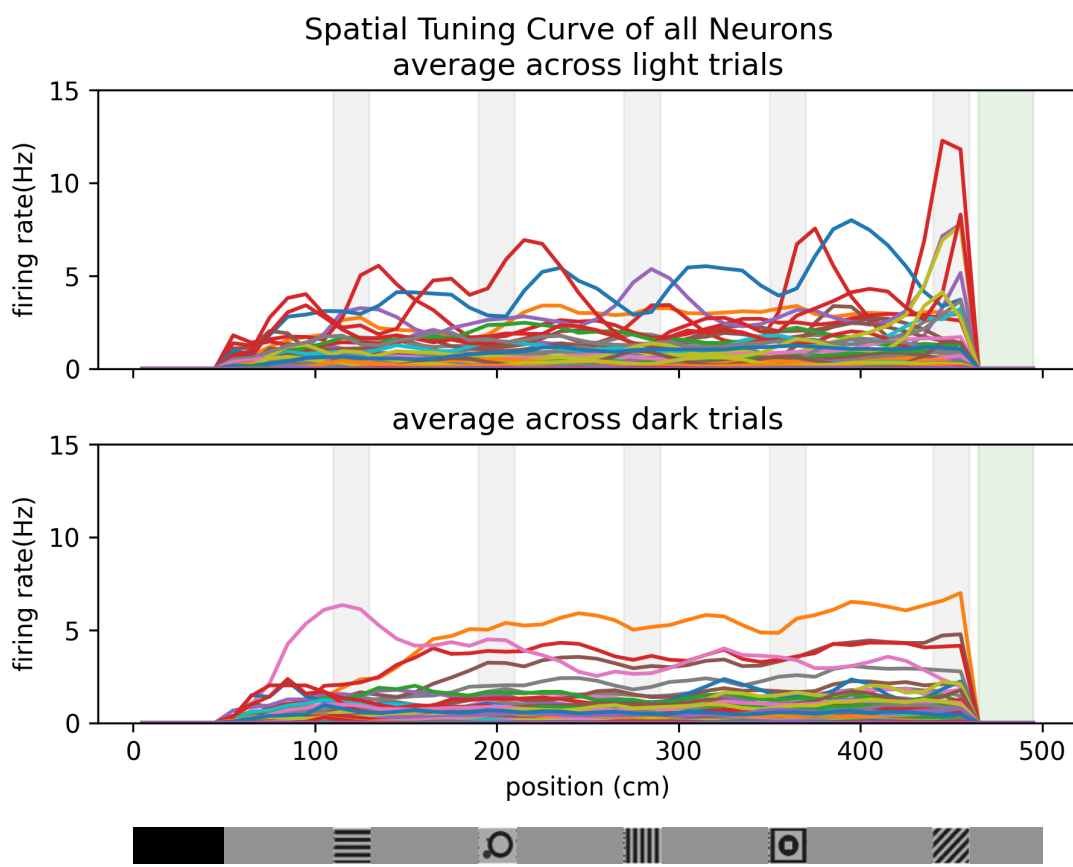


Figure 3: Spatial tuning curves of all recorded neurons from a single mouse

Firing rates from each neuron was averaged across light and dark trials respectively and were plotted as spatial tuning curves. Each line represents the firing rates tuning curve of a recorded neuron ($n = 125$) from the expert mouse. Shaded in grey are the landmarks and shaded in green is the reward zone. Schematic of the virtual tunnel is shown for reference.

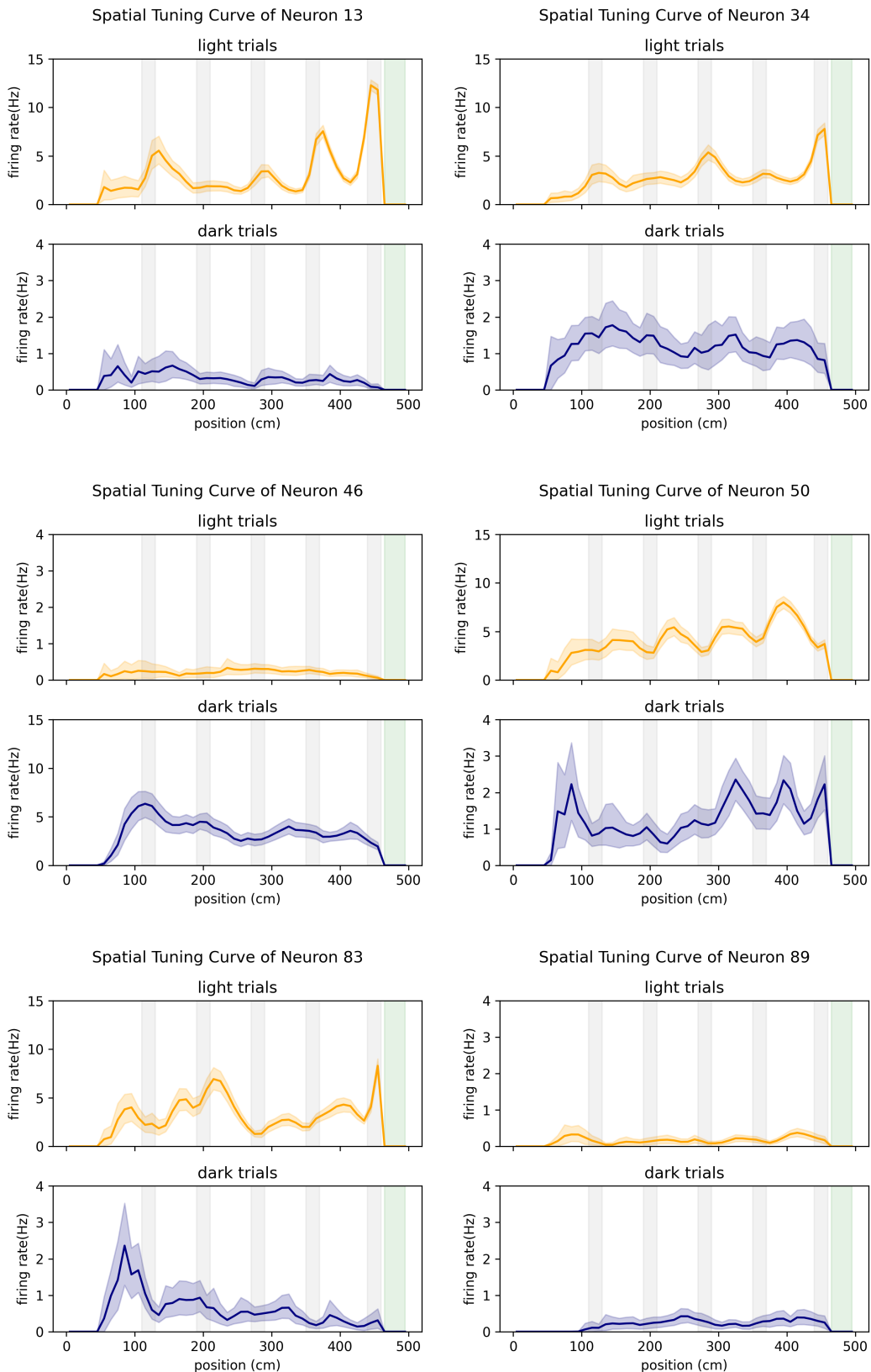


Figure 4: Spatial tuning curves of sample neurons

Firing rates from each neuron was averaged across light and dark trials respectively and were plotted as separate tuning curves (yellow: light, navy: dark). Shaded in grey are the landmarks and shaded in green is the reward zone.

Figure 4 shows the tuning curves of individual neurons across light or dark trials. The majority of neurons did not display heightened activity across spatial positions and were relatively quiet throughout (*e.g.* Neuron 89 in Figure 4). Hence, both light and dark trials have close-to-zero mean firing rates. Most neurons seem to have slightly higher firing rates in light than in dark conditions, with a mean of 0.52 Hz across all neurons and 150 light trials, and a mean of 0.45 Hz across all neurons and 94 dark trials. In rare cases, however, some neurons have higher firing rates in dark trials than in light (*e.g.* Neuron 46).

As seen from the tuning curves, V1 neurons exhibit a variety of spatial tuning properties. Some neurons respond to landmarks while others respond to positions between landmarks or to behavioural-relevant places (*i.e.* reward zone). Finally, other neurons responded to non-spatial behavioural features, such as trial start or reward consumption. For landmark-responsive neurons, some were tuned to specific landmarks, while others (*e.g.* Neuron 50) were tuned to almost every landmark. While in some neurons, the tuning profile in light trials was partially preserved in dark trials (*e.g.* Neuron 13 and Neuron 50), most neurons show different firing patterns in these two conditions.

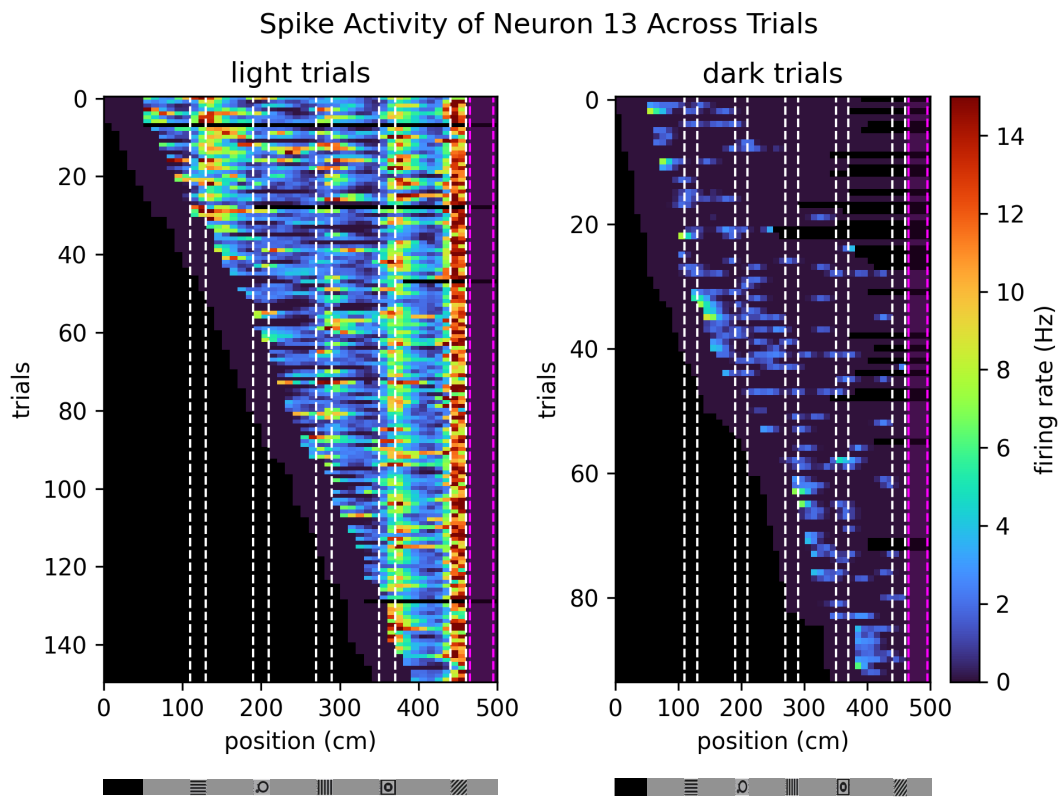


Figure 5: Firing rates heat map of a sample neuron

Firing rates for light and dark trials were sorted by trial start location and plotted separately (150 light trials, 94 dark trials). White dashed lines indicate the landmarks and magenta dashed lines indicate the reward zone. Schematic of the virtual tunnel is shown for reference.

To examine how the firing rates spatial tuning manifest across different trials, single neuron firing rate heatmaps were plotted (Figure 5). As shown in the example neuron, spatial tuning was consistent across light trials despite having different start locations in the virtual tunnel, but it was not stable across dark trials.

3.2. Bayesian Decoder Performance

Is there a spatial representation in mouse V1 during the navigation task in light and dark? To assess the spatial information content of V1 responses, we designed and trained a Bayesian decoder. This decoder would predict the most likely position of the animal at any given temporal bin, based on the activity of V1 neurons. If V1 responses encode the location of the animal within the environment, the decoder should perform above chance.

3.2.1. Assessing the presence of spatial representation in V1

To test whether V1 encodes space in light and dark, the decoder was implemented for light and dark trials independently, and the resulting confusion matrices were examined (Figure 6). Within a confusion matrix, the virtual tunnel is divided into 10 cm position bins. Each row represents the true position of the animal, and each column represents the decoder's predicted position of the animal. The confusion matrix depicts the percentage of the predicted position bin x over all predictions made for true position bin y .

When the decoder was trained from light trial data and tested on light trial data, the confusion matrix shows a clear diagonal from the top left corner to the bottom right, indicating that the decoder made more predictions for the correct position than all other position bins. This was especially clear for the third landmark and the last landmark. The decoder performed best for the position bin closest to the reward zone, where it made a correct prediction 53.77% of the time. This clearly shows that V1 encodes animal surrounds when they are visible as expected.

When the decoder was trained from dark trial data and tested on dark trial data, the confusion matrix no longer shows a clear diagonal. While the decoder did seem to make correct predictions for the beginning of the tunnel, they have become less precise with a wider spread from the diagonal. From the second landmark onwards, the decoder seemed unable to identify where the animal was at all and often predicted the

last position of the tunnel (as seen from the higher values in the last column). This indicates that V1 may not encode animal position in the dark, at least not with the precision compared to that observed for light trials. Alternatively, it may reflect that the current decoder is sub-optimal and thus unable to extract this information from V1 responses.

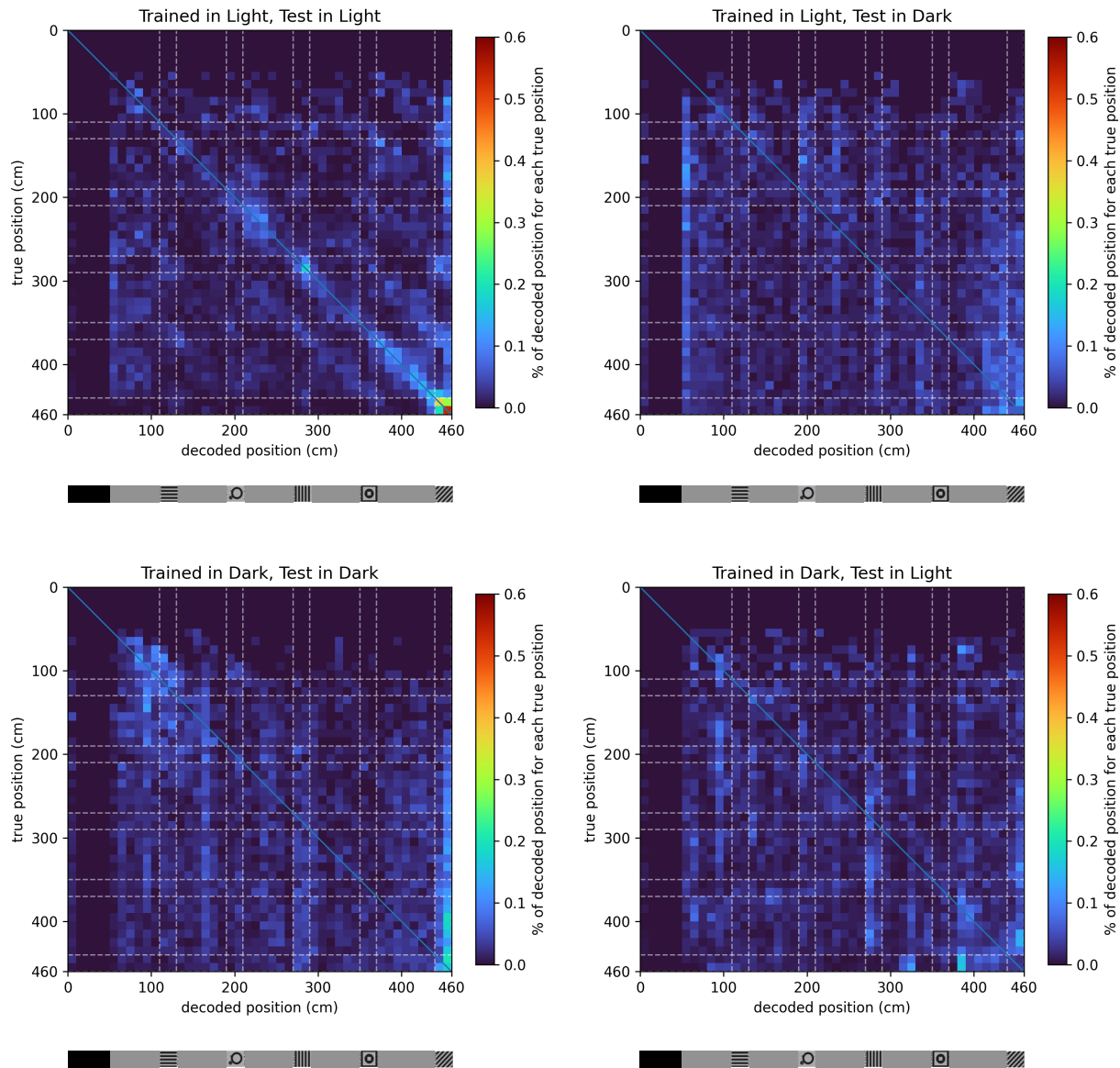
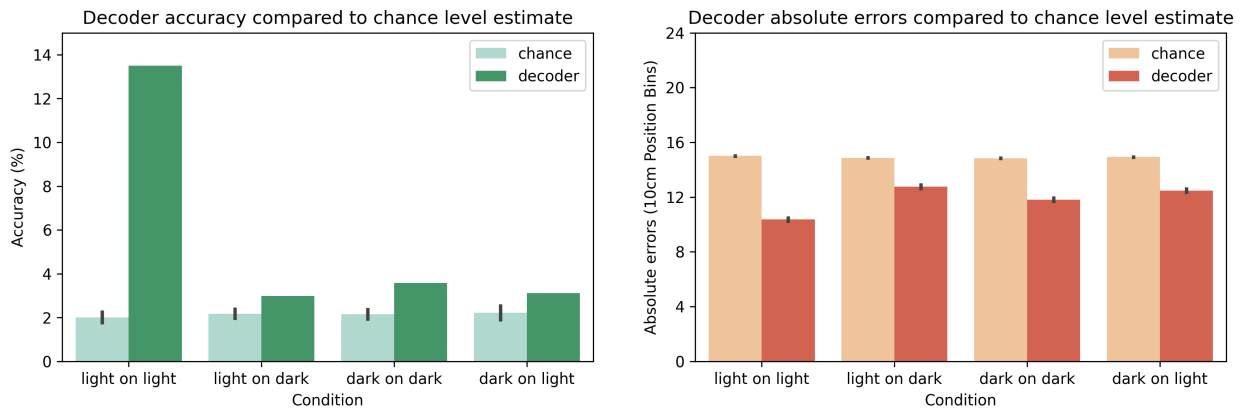


Figure 6: Confusion matrices between decoded position and true position across training paradigms

In the confusion matrices, the virtual tunnel is divided into 10 cm position bins. Each row represents the true position of the animal, and each column represents the decoder's predicted position of the animal. The confusion matrix depicts the percentage of the predicted position bin x over all predictions made for true position bin y . Grey dashed lines indicate the landmarks. Blue diagonal line depicts the ideal where predicted position = true position. Schematic of the virtual tunnel is shown for reference.

The decoder was then evaluated by the accuracy of its predictions against chance level estimates (Figure 7). In both light and dark training paradigms, the decoder performed above the chance level. When trained in light and tested in light, the decoder achieved 13.50% accuracy, more than six times higher than the chance level and is outside the 99% confidence interval for a chance distribution ($2.01\% + 3 \text{ SD} = 2.71\%$). When trained in dark and tested in dark, the decoder achieved 3.58% accuracy, which is also outside the 99% confidence interval for a chance distribution ($2.15\% + 3 \text{ SD} = 2.80\%$). However, this performance was lower than that of the Maximum Likelihood Decoder (Table 3).

The absolute errors of the decoder were also computed as a performance measure (Figure 7). Decoder errors are defined as the absolute distance between the occupied



position bin and the position bin predicted by the decoder. In both light and dark training paradigms, the decoder had smaller errors than the chance level but bigger than that of the Maximum Likelihood Decoder (Table 3).

Figure 7: Decoder accuracy and errors compared to chance level estimate across training paradigms

For each training paradigm, accuracy of the decoder is a single value computed by the number of correct predictions over all predictions (error bar = standard deviation). Errors is the mean of absolute errors between the predicted positions and true positions (error bar = standard error of the mean). For both accuracy and errors, chance level estimates are derived by shuffling the inferred spikes data and feeding the shuffled data to the decoder for 100 repetitions. Accuracy and error values from each of the repetition was aggregated and plotted above.

3.2.2. Assessing similarity and differences between the spatial neural code in light and dark

In addition to evaluating the spatial representations in light and dark, we can also use the decoder to assess whether V1 had similar encoding of space in light and dark

conditions. For this purpose, we trained the decoder with light data and decoded dark responses and vice-versa (cross-training). If V1 spatial encoding in these two conditions were similar, the decoder should perform above chance.

Table 3: Comparison of Accuracy and Errors between Bayesian Decoder and Maximum Likelihood Decoder

Training and Testing Paradigms	Bayesian Decoder		Maximum Likelihood Decoder
	Performance	Chance Level	Performance
Mean Accuracy (%)			
Train in Light, Test in Light	13.50	2.01	16.21
Train in Light, Test in Dark	2.99	2.17	6.81
Train in Dark, Test in Dark	3.58	2.15	11.20
Train in Dark, Test in Light	3.11	2.22	5.51
Mean Absolute Errors (10cm position bins)			
Train in Light, Test in Light	10.36	15.01	5.34
Train in Light, Test in Dark	12.77	14.87	7.24
Train in Dark, Test in Dark	11.81	14.84	4.60
Train in Dark, Test in Light	12.48	14.93	7.61

Training in light and testing in dark achieved above-chance level accuracy 2.99%, which is outside the 99% confidence interval for a chance distribution ($2.17\% + 3 \text{ SD} = 2.79\%$). Training in dark and testing in light also achieved above-chance level accuracy 3.11%, which is also outside the 95% confidence interval for a chance distribution ($2.22\% + 2 \text{ SD} = 2.86\%$).

Observing from the confusion matrices, however, the decoder was unable to make any correct predictions in cross-training paradigms, despite having better-than-chance accuracy and errors. Instead, it seems to have preferences towards certain locations in the tunnel. For example, when training in light and testing in dark, the decoder was biased towards the first position bin of the tunnel. When training in dark and testing in light, the decoder was biased toward the third landmark. Once again, this may mean that the encoding of space in V1 in light and dark trials, if present, is different for each condition. Alternatively, it may also mean that the decoder requires further optimization to reveal a shared code.

3.2.3. Evaluating certainty of the decoder

Finally, the decoder was evaluated by how certain it was about its predictions. When the decoder makes a prediction, it scans through all the positions and finds the position bin with the maximum posterior probability. The maximum posterior probability is how “certain” the decoder is. Figure 8 plots the joint distribution between the certainty of the decoder and the decoded positions.

When decoding light trial data, the decoder became more certain (having higher maximum posterior probabilities) towards the end of the tunnel where the animal is closest to the reward zone. This is in line with the confusion matrix for training in light and testing in light, where the predictions closest to the reward zone were the most accurate.

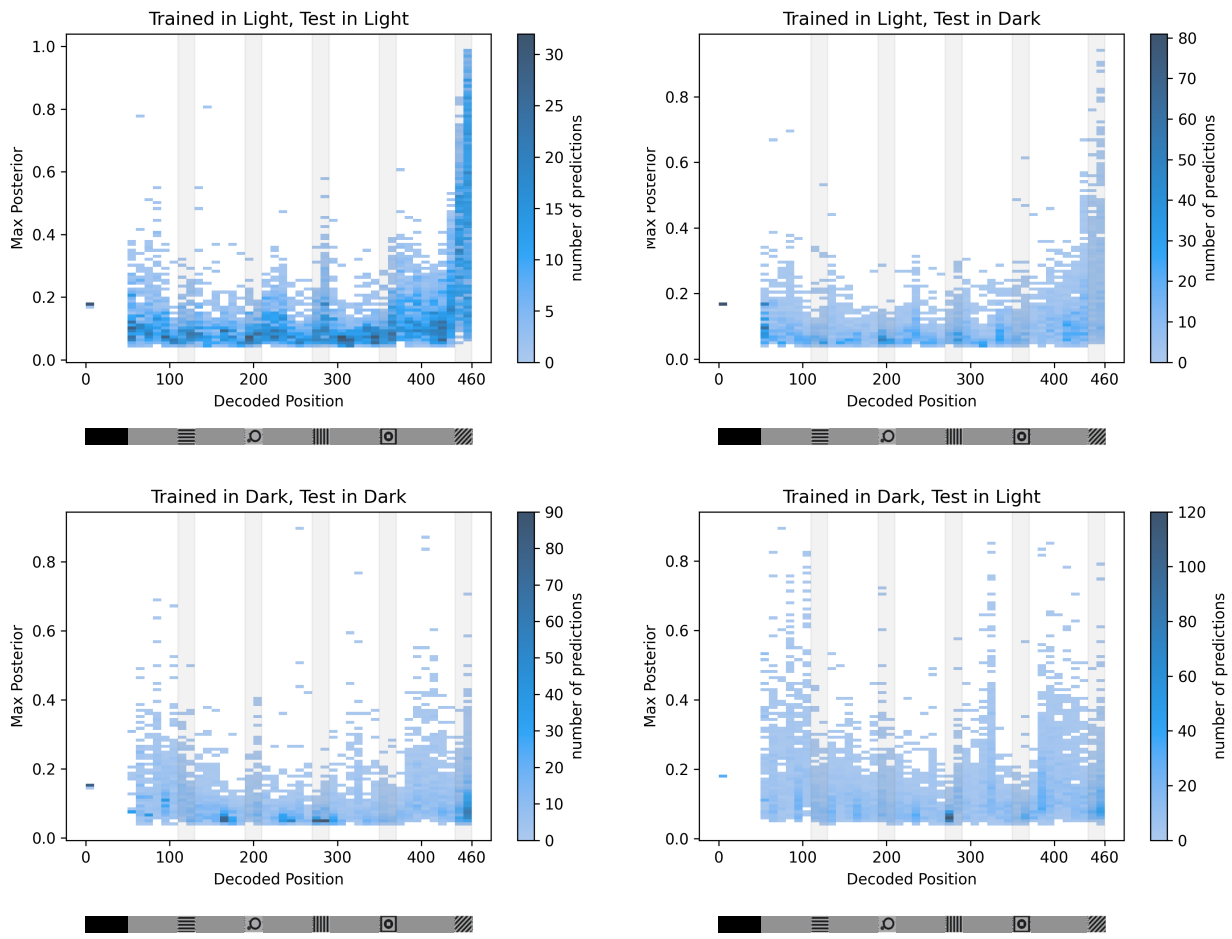


Figure 8: Joint distributions of decoder certainty and decoded position across training paradigms

The maximum posterior probability is taken as “certainty” of the decoder. Higher max posterior probability indicates the decoder was more certain about that particular prediction. Shaded in grey are the landmark locations. Schematic of the virtual tunnel is shown for reference.

When decoding dark trials data, the decoder had higher certainty for its predictions in the beginning and the end of the tunnel, but lower certainty for the middle of the tunnel. This is also in line with the confusion matrix for training in dark and testing in dark, where the decoder shows bias towards the beginning of the tunnel and the last position of the tunnel. It also made more correct predictions for the beginning and the end of the tunnel.

3.3. Results Conclusion

Altogether, these results indicate that despite not showing great precision in predicting the animal's position, as shown in the overall accuracy, errors, and confusion matrices, the decoder outperformed chance, suggesting that spatial information seems to be encoded in V1 during light navigation and, to a lesser degree, during dark navigation, for the single expert mouse used to develop this method.

The overall low decoder performance, as compared to the Maximum Likelihood Decoder, likely has to do with technical limitations in the decoding strategy that prevented the decoder from extracting the right information encoded in V1, as suggested by the generally low certainty levels of the decoder. Thus, future efforts will focus on optimising this strategy as discussed in the next section.

4. Discussion

Reliable spatial representations are critical for navigation in a familiar environment especially when visual cues are lacking in the dark. However, how these internal representations of the environment are recruited in the absence of visual cues and whether they propagate down to the primary visual cortex remains unclear.

This thesis hypothesised that spatial representations are encoded in V1 both in light and in dark when visual cues are absent. In addressing the hypothesis, a Bayesian decoder was developed to predict the spatial location of the animal from its neuronal activity. The decoder was implemented using V1 neural responses of one expert mouse during a virtual reality navigation task. Despite technical limitations and the use of data from only a single mouse, the results demonstrated that the decoder outperformed chance level, offering preliminary support to the hypothesis that spatial representations are encoded in V1 both in light and dark.

4.1. Advantages and limitations of Bayesian Decoder

4.1.1. Advantages of adopting Bayesian inference

This thesis proposed the use of Bayesian inference because of its ability to account for uncertainty in position predictions given limited and noisy data. The decoder was able to outperform chance in all measures and across all training paradigms, even in situations where spatial representations in neural tuning curves were not pronounced (in the dark), and where the sharing of spatial neural code between light and dark was under question (in the cross-training paradigms). Such performance was achieved by the decoder despite the small fraction of spatially tuned neurons in V1 in darkness. The probabilistic output of the decoder also provided a “confidence” level of its predictions, which made it possible to evaluate the quality of decoder predictions.

4.1.2. Limitations and optimisation for decoder

Despite the advantages, the heterogeneity in trial structure presents a major challenge for the decoder, which contributes to the sub-optimal performance of the decoder.

Firstly, confounding factors that come from the variable trial lengths might decrease decoder performance. As previously reviewed (Flossmann and Rochefort, 2021), V1 response could integrate other navigational signals such as distance travelled, travelling speed, and licking events. These confounding behavioural variables vary across trials with different lengths, thus V1 could respond differently to the same position in a short trial compared to a long trial. To assess whether neural code in V1 contains these auxiliary variables, future iterations of the decoder can group trials of similar lengths and decode each group separately to exploit encoding of distance.

The second adjustment is to vary the spatial prior by trial length. As explained in the Introduction, priors help improve Bayesian decoder accuracy by incorporating known information or hypotheses. Out of simplicity, the current spatial prior is uniform across trials, which does not reflect the actual task structure. By varying the spatial prior according to trial length, this provides additional information for the decoder to refine its predictions. The second adjustment that can be made is to increase the time bin size of the data from 100 ms to 200 ms. By doubling the time bin size, the noise in the data would be dampened and produce a more pronounced signal-to-noise ratio (Zhang et al., 1998).

4.2. Decoder performance and spatial neural code

4.2.1. Spatial representation in mouse V1 in light and dark

To test whether V1 encodes space in light and dark, the decoder was implemented for light and dark trials independently and the preliminary results suggested that while spatial representation exists in light, it was not obvious from the tuning curves of individual neurons whether it is preserved in the dark.

In light, the resulting confusion matrix has a clear diagonal, indicating that the decoder could make correct predictions of the mouse location based on its neuronal activity. The accuracy of the decoder was six times above chance level, and the absolute errors were below chance as well. Altogether, these results suggested that spatial representations were encoded in V1, which has been demonstrated in the previous literature (Fiser et al., 2016; Pakan et al., 2018; Saleem et al., 2018).

However, results were much less conclusive in the dark. On one hand, the confusion matrix in dark did not have a clear diagonal, and the spatial tuning for each neuron in

dark was not stable across trials, suggesting that there were no spatial representations from the neuronal activity. On the other hand, the decoder did outperform chance in dark for both accuracy and absolute errors, suggesting that spatial representations were not completely absent in the dark.

There are several possibilities for these seemingly contradicting results in the dark. First, the lack of clear diagonal in the confusion matrix could come from the degrading of spatial representations in the dark. Researchers have previously shown that hippocampal spatial information would degrade in the dark if there was no feedback from other sensory inputs (Zhang et al., 2014). In other words, the spatial representations could be present initially but failed to be maintained throughout the whole trial. This might explain why the decoder could still outperform chance despite not having a clear confusion matrix as there was still a small amount of spatial information available at the beginning of the trial.

Confounding factors that come from the variable trial lengths, such as distance travelled and lick events, might also contribute to these contradicting results. They could influence V1 to respond differently to the same position in trials of different lengths, which might explain why the spatial tuning in dark was unstable across trials.

To verify the preliminary results from this thesis, the decoder should be optimised to make use of these additional factors (e.g. distance travelled) and applied to data from other expert animals in the future.

4.2.2. Sharing of spatial neural code between light and dark

To evaluate if the spatial neural code between light and dark was shared, the decoder was cross-trained in light data and tested in dark data (and vice versa). While the decoder outperformed chance in accuracy and absolute errors for the cross-trained paradigms, the confusion matrices suggested that the decoder was not able to make correct predictions reliably. This could mean that the spatial neural code was not shared between light and dark. However, to avoid concluding prematurely, the decoder can be further optimised with the incorporation of dimensionality reduction techniques such as principal component analysis (PCA).

PCA is a dimensionality reduction technique that aims to capture the high-dimensionality data into low-dimensionality subspaces that could explain the largest variance in the data. One could then compare the subspaces in light trial data and dark

trial data to find any similarities between the spatial neural code in light and dark. One could also utilise the shared latent spatial subspace to improve the decoder performance in cross-trained paradigms.

4.3. Future direction: application to large-scale electrophysiological recordings

While it requires further testing with other expert mice, the results gathered in this thesis provide preliminary support that spatial representations are encoded in V1 in light, and to a smaller extent in dark. Future experiments using large-scale electrophysiological recordings can be conducted to validate if spatial representations are present in the visual cortex in light and dark.

Using data obtained with alternative recording techniques can also help validate the results. Large-scale electrophysiological recordings such as Neuropixel allow researchers to look at neural activity with higher temporal resolutions. It also allows researchers to record neuronal spikes directly, which improves signal-to-noise and prevents the need for complicated pre-processing pipelines that might cause information to be lost. Lastly, the use of Neuropixel probes provides more flexibility in experimental design. For example, researchers can conduct recordings in multiple regions of interest. This is particularly useful for future experiments to determine the cortical circuits responsible for conveying spatial information from higher cortical areas to V1. This can be done through the simultaneous recording of V1 and RSC or MEC using multiple Neuropixel probes. The use of Neuropixel can also be adapted for freely moving animals, which could allow researchers to explore spatial representations in the dark without head fixation.

As large-scale electrophysiological recording technology continues to become more accessible, the Bayesian decoding methodology developed from this thesis could readily adapt and provide a powerful tool for analysing data collected from these electrophysiological recordings.

References

- Barrett LF, Simmons WK (2015) Interoceptive predictions in the brain. *Nature Reviews Neuroscience* 16:419–429
- Campbell MG, Attinger A, Ocko SA, Ganguli S, Giocomo LM (2021) Distance-tuned neurons drive specialized path integration calculations in medial entorhinal cortex. *Cell Reports* 36:109669.
- Clark A (2013) Whatever next? Predictive brains, situated agents, and the future of cognitive science. *Behavioral and Brain Sciences* 36:181–204.
- de Lange FP, Heilbron M, Kok P (2018) How Do Expectations Shape Perception? *Trends in Cognitive Sciences* 22:764–779.
- Elduayen C, Save E (2014) The retrosplenial cortex is necessary for path integration in the dark. *Behavioural Brain Research* 272:303–307.
- Etter G, Manseau F, Williams S (2020) A Probabilistic Framework for Decoding Behavior From in vivo Calcium Imaging Data. *Frontiers in Neural Circuits* 14.
- Fischer LF, Mojica Soto-Albors R, Buck F, Harnett MT (2020) Representation of visual landmarks in retrosplenial cortex. *eLife* 9.
- Fiser A, Mahringer D, Oyibo HK, Petersen AV, Leinweber M, Keller GB (2016) Experience-dependent spatial expectations in mouse visual cortex. *Nature Neuroscience* 19:1658–1664.
- Flossmann T, Rochefort NL (2021) Spatial navigation signals in rodent visual cortex. *Current Opinion in Neurobiology* 67:163–173.
- Friston K (2005) A theory of cortical responses. *Philosophical Transactions of the Royal Society B: Biological Sciences* 360:815–836.
- Gerlei KZ, Brown CM, Sürmeli G, Nolan MF (2021) Deep entorhinal cortex: from circuit organization to spatial cognition and memory. *Trends in Neurosciences* 44:876–887.

- Gobbo F, Mitchell-Heggs R, Tse D, Al Omrani M, Spooner PA, Schultz SR, Morris RGM (2022) Neuronal signature of spatial decision-making during navigation by freely moving rats by using calcium imaging. *Proceedings of the National Academy of Sciences* 119.
- Gramann K, Onton J, Riccobon D, Mueller HJ, Bardins S, Makeig S (2010) Human Brain Dynamics Accompanying Use of Egocentric and Allocentric Reference Frames during Navigation. *Journal of Cognitive Neuroscience* 22:2836–2849.
- Grosmark AD, Buzsaki G (2016) Diversity in neural firing dynamics supports both rigid and learned hippocampal sequences. *Science* 351:1440–1443.
- Huang R-S, Sereno MI (2013) Bottom-up Retinotopic Organization Supports Top-down Mental Imagery. *The Open Neuroimaging Journal* 7:58–67.
- Keller GB, Mrsic-Flogel TD (2018) Predictive Processing: A Canonical Cortical Computation. *Neuron* 100:424–435.
- Knill DC, Pouget A (2004) The Bayesian brain: the role of uncertainty in neural coding and computation. *Trends in Neurosciences* 27:712–719.
- Kober SE, Wood G, Kampl C, Neuper C, Ischebeck A (2014) Electrophysiological correlates of mental navigation in blind and sighted people. *Behavioural Brain Research* 273:106–115.
- Kwan AC, Dietz SB, Zhong G, Harris-Warrick RM, Webb WW (2010) Spatiotemporal Dynamics of Rhythmic Spinal Interneurons Measured With Two-Photon Calcium Imaging and Coherence Analysis. *Journal of Neurophysiology* 104:3323–3333.
- Lee K, Lee Y, Lin D-T, Bhattacharyya SS, Chen R (2019) Real-Time Calcium Imaging Based Neural Decoding with a Support Vector Machine. In. 2019 IEEE Biomedical Circuits and Systems Conference (BioCAS).
- Lee K, Wu X, Lee Y, Lin D-T, Bhattacharyya SS, Chen R (2020) Neural decoding on imbalanced calcium imaging data with a network of support vector machines. *Advanced Robotics* 35:459–470.
- Lee Y, Sreenuj Chellath Madayambath, Liu Y, Lin D-T, Chen R, Bhattacharyya SS (2017) Online learning in neural decoding using incremental linear discriminant analysis. In. 2017 IEEE International Conference on Cyborg and Bionic Systems (CBS).

- Mao D, Molina LA, Bonin V, McNaughton BL (2020) Vision and Locomotion Combine to Drive Path Integration Sequences in Mouse Retrosplenial Cortex. *Current Biology* 30:1680-1688.e4.
- McNaughton BL, Battaglia FP, Jensen O, Moser EI, Moser M-B (2006) Path integration and the neural basis of the “cognitive map.” *Nature Reviews Neuroscience* 7:663–678.
- Moser EI, Kropff E, Moser M-B (2008) Place Cells, Grid Cells, and the Brain’s Spatial Representation System. *Annual Review of Neuroscience* 31:69–89.
- O’Keefe J, Conway DH (1978) Hippocampal place units in the freely moving rat: Why they fire where they fire. *Experimental Brain Research* 31.
- O’Neill J, Boccara CN, Stella F, Schoenenberger P, Csicsvari J (2017) Superficial layers of the medial entorhinal cortex replay independently of the hippocampus. *Science* 355:184–188.
- Pakan JMP, Currie SP, Fischer L, Rochefort NL (2018) The Impact of Visual Cues, Reward, and Motor Feedback on the Representation of Behaviorally Relevant Spatial Locations in Primary Visual Cortex. *Cell Reports* 24:2521–2528.
- Pfeiffer BE, Foster DJ (2013) Hippocampal place-cell sequences depict future paths to remembered goals. *Nature* 497:74–79.
- Rao RPN, Ballard DH (1999) Predictive coding in the visual cortex: a functional interpretation of some extra-classical receptive-field effects. *Nature Neuroscience* 2:79–87.
- Rupprecht P, Carta S, Hoffmann A, Mayumi Echizen, Blot A, Kwan AC, Dan Y, Hofer SB, Kitamura K, Fritjof Helmchen, Friedrich RW (2021) A database and deep learning toolbox for noise-optimized, generalized spike inference from calcium imaging. *Nature Neuroscience* 24:1324–1337.
- Saleem AB, Diamanti EM, Fournier J, Harris KD, Carandini M (2018) Coherent encoding of subjective spatial position in visual cortex and hippocampus. *Nature* 562:124–127.
- Sun D, Yu Y, Habibollahi F, Unnithan RR, French C (2023) Real-time multimodal sensory detection using widefield hippocampal calcium imaging. *Communications Engineering* 2:1–11.

- Tenant SA, Clark H, Hawes I, Tam WK, Hua J, Yang W, Gerlei KZ, Wood ER, Nolan MF (2022) Spatial representation by ramping activity of neurons in the retrohippocampal cortex. *Current Biology*.
- Tu M, Zhao R, Adler A, Gan W, Chen Z (2020) Efficient Position Decoding Methods Based on Fluorescence Calcium Imaging in the Mouse Hippocampus. *Neural Computation* 32:1144–1167.
- van der Meer MAA, Carey AA, Tanaka Y (2017) Optimizing for generalization in the decoding of internally generated activity in the hippocampus. *Hippocampus* 27:580–595.
- Zhang K, Ginzburg I, McNaughton BL, Sejnowski TJ (1998) Interpreting Neuronal Population Activity by Reconstruction: Unified Framework With Application to Hippocampal Place Cells. *Journal of Neurophysiology* 79:1017–1044.
- Zhang S, Schünfeld F, Wiskott L, Manahan-Vaughan D (2014) Spatial representations of place cells in darkness are supported by path integration and border information. *Frontiers in Behavioral Neuroscience* 8.
- Zhu L, Lee CR, Margolis DJ, Najafizadeh L (2018) Decoding cortical brain states from widefield calcium imaging data using visibility graph. *Biomedical Optics Express* 9:3017.